

Cite this: *Chem. Sci.*, 2017, 8, 5434

## Electrocatalytic synthesis of ammonia by surface proton hopping†

R. Manabe,<sup>a</sup> H. Nakatsubo,<sup>a</sup> A. Gondo,<sup>a</sup> K. Murakami,<sup>a</sup> S. Ogo,<sup>a</sup> H. Tsuneki,<sup>b</sup> M. Ikeda,<sup>b</sup> A. Ishikawa,<sup>c</sup> H. Nakai<sup>cd</sup> and Y. Sekine<sup>id</sup>\*<sup>a</sup>

Highly efficient ammonia synthesis at a low temperature is desirable for future energy and material sources. We accomplished efficient electrocatalytic low-temperature ammonia synthesis with the highest yield ever reported. The maximum ammonia synthesis rate was 30 099  $\mu\text{mol g}_{\text{cat}}^{-1} \text{h}^{-1}$  over a 9.9 wt% Cs/5.0 wt% Ru/SrZrO<sub>3</sub> catalyst, which is a very high rate. Proton hopping on the surface of the heterogeneous catalyst played an important role in the reaction, revealed by *in situ* IR measurements. Hopping protons activate N<sub>2</sub> even at low temperatures, and they moderate the harsh reaction condition requirements. Application of an electric field to the catalyst resulted in a drastic decrease in the apparent activation energy from 121 kJ mol<sup>-1</sup> to 37 kJ mol<sup>-1</sup>. N<sub>2</sub> dissociative adsorption is markedly promoted by the application of the electric field, as evidenced by DFT calculations. The process described herein opens the door for small-scale, on-demand ammonia synthesis.

Received 22nd February 2017  
Accepted 20th May 2017

DOI: 10.1039/c7sc00840f

rsc.li/chemical-science

## Introduction

Ammonia is an important compound that is widely used as a raw material for chemical fertilizers, fibers, resins and refrigerants. Recently, ammonia has been suggested as a hydrogen carrier because of its high hydrogen content.<sup>1</sup> At present, the Haber–Bosch process using nitrogen and hydrogen is the main method for ammonia synthesis. This process is conducted at high pressures (over 200 atm) and high reaction temperatures (around 773 K) because of its thermodynamic and kinetic limitations.<sup>2</sup> For this reason, the energy consumption for ammonia synthesis is very large.<sup>3</sup> Smaller scale, more dispersed ammonia plants could be developed if an ammonia synthesis route with milder operating conditions is realized. To date, numerous investigations into high-efficiency ammonia synthesis using milder operating conditions have been conducted. The original ammonia synthesis catalyst was an Fe-based double promotion catalyst.<sup>4</sup> In 1972, Aika *et al.* reported a supported Ru catalyst<sup>5</sup> that showed high activity for ammonia synthesis. This discovery of a Ru catalyst with alkali metals as co-catalysts<sup>6–11</sup> led to a decrease in the reaction temperatures and pressures necessary for Haber–Bosch processing. Recently, Ru catalysts supported on praseodymium oxide,<sup>12</sup> electride catalysts,<sup>13–15</sup> and calcium amide<sup>16</sup> have shown high ammonia

synthesis rates, even at pressures and temperatures as low as 0.1 MPa and 600–700 K. In addition, ammonia synthesis at room temperature (around 298 K) and atmospheric pressure can be achieved using metal complexes including molybdenum,<sup>17,18</sup> iron<sup>19</sup> and cobalt,<sup>20</sup> as well as with a titanium hydride compound.<sup>21</sup> Moreover, examples of ammonia synthesis routes using an external DC electric field,<sup>22</sup> plasma,<sup>23–28</sup> photocatalysis<sup>29</sup> and electrolysis<sup>30</sup> have been reported, which indicate the possibility of low-temperature ammonia synthesis by exploiting the synergy between electrical/photochemical processes and catalysis. However, the ammonia synthesis rates using these methods are hindered by kinetic limitations. The present work proposes a new catalytic ammonia synthesis process assisted by an electric field which can show a high ammonia synthesis rate even at low temperatures. We achieved ammonia synthesis under very mild conditions (room temperature and pressures ranging from atmospheric up to 0.9 MPa) using a Ru–Cs catalyst. The process is more efficient than electrolytic synthesis because the process is non-faradaic ( $\lambda > 50$ ). The process is also different from that using plasma, as it is conducted under much milder conditions with lower electric power consumption. This process is not intended as a replacement for the Haber–Bosch process, but rather for the creation of new uses and demand. Using this method of ammonia synthesis, highly pure ammonia can be collected as a compressed liquid by virtue of the extremely low reaction temperature. Therefore, small-scale and efficient processes for ammonia synthesis can be realized by application of an electric field.

<sup>a</sup>Department of Applied Chemistry, Waseda University, 3-4-1, Okubo, Shinjuku, Tokyo 169-8555, Japan. E-mail: ysekine@waseda.jp<sup>b</sup>Nippon Shokubai Co. Ltd., 5-8, Nishiotabi, Suita, Osaka 564-0034, Japan<sup>c</sup>Department of Chemistry and Biochemistry, Waseda Univ., Japan<sup>d</sup>ESICB, Kyoto University, Kyoto-daigaku-katsura, Kyoto, 615-8520 Japan

† Electronic supplementary information (ESI) available. See DOI: 10.1039/c7sc00840f

## Results and discussion

### Kinetic analyses for catalytic ammonia synthesis in an electric field

We conducted pre-screening tests for this purpose (results not shown), and we found that 9.9 wt% Cs/5.0 wt% Ru/SrZrO<sub>3</sub> showed high activity for ammonia synthesis in an electric field, even at low reaction temperatures in the range of 463–634 K and pressures from atmospheric to 0.9 MPa, as presented in Fig. 1(A). We obtained a remarkably high ammonia yield, with an ammonia production rate as high as 30 099  $\mu\text{mol g}_{\text{cat}}^{-1} \text{h}^{-1}$  at 0.9 MPa, which is still in the kinetically controlled region. Interestingly, this impressive activity was also stable for 5 h. The application of an electric field increased the activity drastically, irrespective of the state of pressurization. The energy consumption was very low (only 2.82 W), and the ammonia production energy efficiency of 36.3 g kW h<sup>-1</sup> is the highest ever reported. The faradaic efficiency (*i.e.* the ratio between the molar amounts of NH<sub>3</sub> produced and electrons consumed) was as high as 26.88, strongly indicating that the reaction is non-faradaic. Interestingly, the pressure effects were more pronounced when the reaction proceeded under the influence of an electric field.

To elucidate the mechanism behind the electric field effect on catalytic ammonia synthesis, we conducted detailed kinetic analyses of the reaction. Fig. 1(B) presents Arrhenius plots for the ammonia synthesis reaction in the kinetic regime under both atmospheric and elevated pressure. The apparent activation energy decreased from 121 kJ mol<sup>-1</sup> to 37 kJ mol<sup>-1</sup> upon applying the electric field at 0.9 MPa. These results suggest that the ammonia synthesis reaction mechanism is affected by the electric field, and that the rate-determining step of the reaction changes.

To gain further mechanistic information, the N<sub>2</sub>, H<sub>2</sub> and NH<sub>3</sub> pressure dependencies of the ammonia synthesis rate were investigated. The obtained results are presented in Table S1 of

the ESI.† With the assumption that the rate of the ammonia synthesis reaction can be written as in eqn (1), eqn (2)–(5) were used for kinetic analyses:<sup>31,32</sup>

$$r = k P_{\text{N}_2}^{\alpha} P_{\text{H}_2}^{\beta} P_{\text{NH}_3}^{\gamma} \quad (1)$$

$$r = W^{-1} dy_0/d(1/q) \quad (2)$$

$$\log y_0 = \log(c/q)^{1/m} \quad (3)$$

$$r = W^{-1} c/m y_0^{(1-m)} \quad (4)$$

$$c = k' P_{\text{N}_2}^{\alpha} P_{\text{H}_2}^{\beta}, \quad (5)$$

where  $r$  stands for the reaction rate of the ammonia synthesis,  $W$  denotes the catalyst weight,  $y_0$  signifies the ammonia mole fraction,  $q$  represents the mass flow and  $(1 - m)$  corresponds to  $\gamma$ .

As shown in Table S1,† for the catalytic reaction (without the electric field), the ammonia synthesis rate exhibited a positive N<sub>2</sub> partial pressure dependence with an order of 0.68. However, the H<sub>2</sub> and NH<sub>3</sub> partial pressure dependencies of the reaction rate were negative (−0.21 for H<sub>2</sub> and −0.1 for NH<sub>3</sub>). These trends are in excellent agreement with past kinetic studies of ammonia synthesis.<sup>8,11,32,33</sup> They indicated that the rate-determining steps of the catalytic reaction without the electric field include N<sub>2</sub> activation, especially N<sub>2</sub> dissociative adsorption on Ru, because of the strong triple bond energy of N<sub>2</sub>. However, when the catalyst included an electron donor such as Cs, the reaction order of N<sub>2</sub> became smaller than unity, at around 0.7.<sup>8</sup> In addition, the negative H<sub>2</sub> pressure dependence indicates that the surface of Ru was poisoned by hydrogen. On the other hand, upon application of the electric field, the N<sub>2</sub> and H<sub>2</sub> pressure dependencies of the ammonia synthesis rate changed drastically. The N<sub>2</sub> pressure dependence of the reaction rate decreased upon applying the electric field, indicating that the N<sub>2</sub> activation steps were promoted by the electric field. In addition, the H<sub>2</sub> pressure dependence of the reaction rate weakened; the reaction orders were 0.24 for N<sub>2</sub>, 0 for H<sub>2</sub> and −0.26 for NH<sub>3</sub>. Therefore, the poisoning of Ru by hydrogen disappeared to some extent upon application of the electric field.

To specifically examine the effect of the electric field on N<sub>2</sub> activation, isotope exchange tests were conducted using <sup>30</sup>N<sub>2</sub>. Fig. 2 presents the results obtained in transient response tests using <sup>28</sup>N<sub>2</sub> and switching to <sup>30</sup>N<sub>2</sub>. When <sup>30</sup>N<sub>2</sub> was supplied in the presence of the electric field at 473 K, <sup>29</sup>N<sub>2</sub> formation was observed. However, without the electric field, <sup>29</sup>N<sub>2</sub> was not detected, even at higher reaction temperatures, as shown in Fig. 2 ( $T \leq 673$  K). Generally, the isotope exchange tests using <sup>30</sup>N<sub>2</sub> were conducted while only supplying N<sub>2</sub> species to avoid H<sub>2</sub> poisoning of the Ru surface.<sup>34</sup> In our isotopic tests without supplying H<sub>2</sub> and without application of the electric field, <sup>29</sup>N<sub>2</sub> was not detected either, even at 873 K (Fig. S1†). In addition, H<sub>2</sub> was necessary for the isotopic tests when applying the electric field because without a hydrogen supply, application of the electric field resulted in a spark discharge. This phenomenon demonstrates that hydrogen, or a chemical compound

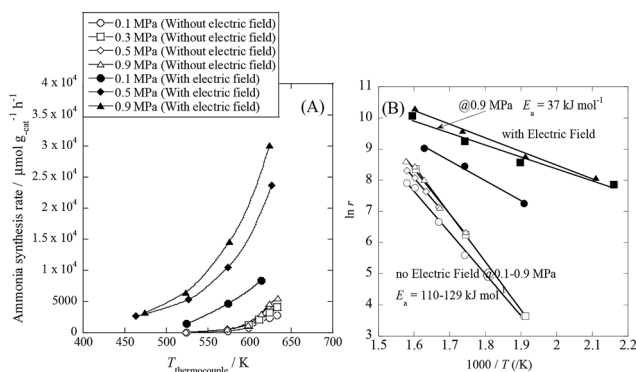


Fig. 1 Temperature and pressure dependence of ammonia synthesis activity with or without an electric field. (A) Temperature dependence of the ammonia synthesis rate at various pressures, with or without an electric field. (B) Arrhenius plots for each reaction under various pressures in the kinetic regime: catalyst bed temperature, 463–634 K; catalyst, 9.9 wt% Cs/5.0 wt% Ru/SrZrO<sub>3</sub>, 200 mg; flow, N<sub>2</sub> : H<sub>2</sub> = 60 : 180 SCCM; current, 0 or 6 mA.



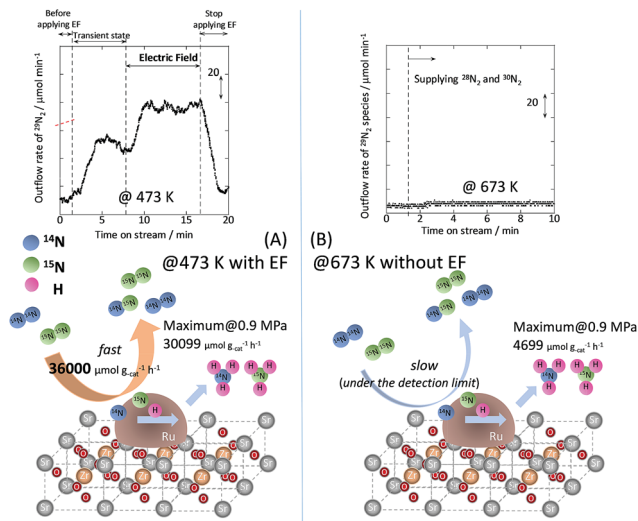
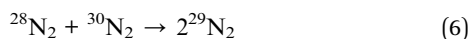


Fig. 2 Isotope exchange tests using  $^{30}\text{N}_2$ , (A) with an electric field at 473 K, and (B) without an electric field at 673 K. Catalyst, 9.9 wt% Cs/5.0 wt% Ru/SrZrO<sub>3</sub>, 200 mg; flow,  $^{28}\text{N}_2$  :  $^{30}\text{N}_2$  :  $\text{H}_2$  : Ar = 6 : 6 : 36 : 12 SCCM; current, 0 or 6 mA.

containing hydrogen, plays the role of an ion carrier, enabling the stable application of the electric field.

As shown in eqn (6),  $^{29}\text{N}_2$  was produced through the dissociative adsorption of  $^{28}\text{N}_2$  and  $^{30}\text{N}_2$ , followed by the recombination of  $^{28}\text{N}_2$  and  $^{30}\text{N}_2$ . The  $\text{N}_2$  dissociation rate can therefore be calculated from the  $^{29}\text{N}_2$  production rate, using eqn (7)–(9), assuming steady-state conditions at the surface of the catalyst:<sup>34,35</sup>



The balance equation for N species flow is

$$V_{\text{in}} - V_{\text{out}} - r_{\text{NH}_3}/2 = 0 \quad (7)$$

and the equations for  $\text{N}_2$  outflow are

$$F_{28} = (F_{28})_0 + V_{\text{out}} \times (f_{s14}f_{s14}) - V_{\text{in}} \times (f_{28})_0 \quad (8)$$

and

$$F_{29} = V_{\text{out}} \times (2f_{s14}f_{s15}) = V_{\text{out}} \times \{2f_{s14} \times (1 - f_{s14})\}, \quad (9)$$

where  $V$  signifies the total flow rate,  $F$  denotes the flow of each species, and  $f$  represents the mole fraction of the isotopic species. Subscripts 28, 29, 14 and 15 respectively denote  $^{28}\text{N}_2$ ,  $^{29}\text{N}_2$ ,  $^{14}\text{N}$  and  $^{15}\text{N}$ , subscript s signifies the Ru surface, and subscript 0 denotes an input value (detailed procedures are presented in the ESI†). From the calculation, the  $\text{N}_2$  dissociation rate per gram of catalyst was about  $36\,000\,\mu\text{mol g}^{-1}\text{h}^{-1}$  when applying the electric field at 473 K. However, the  $\text{N}_2$  dissociation rate could not be calculated for the catalytic reaction because  $^{29}\text{N}_2$  was below the limit of detection. These results indicate that  $\text{N}_2$  dissociative adsorption is very rapid and is enhanced irreversibly in the electric field.

## In situ DRIFTS measurements

To observe the adsorbed species on the surface of the catalyst during application of the electric field for ammonia synthesis, and to reveal the mechanism of the ammonia synthesis reaction in the presence of the electric field, *in situ* diffuse reflectance infrared Fourier transform spectroscopy (DRIFTS) measurements were conducted. With a customized cell, we measured the IR spectrum when the electric field was applied to the catalyst bed, as presented in Fig. S2.† The obtained *in situ* DRIFTS spectra under each condition are shown in Fig. 3. Assignments are presented in the table in Fig. 3. As shown in Fig. 3(A), no peaks were observed when supplying only  $\text{N}_2$  and  $\text{H}_2$  at 473 K. However, when applying the electric field, four sharp peaks around  $3146$ ,  $3046$ ,  $2819$  and  $1406\text{ cm}^{-1}$  were detected. These peaks were not observed under a pure  $\text{N}_2$  supply with the electric field (C), or during ammonia synthesis at  $648\text{ K}$  without the electric field (D). Therefore, these four peaks were observed only when the electric field was applied to the catalyst bed. They were assigned to the stretching, combination tone, overtone and bending modes of N–H vibrations derived from  $\text{NH}_4^+$ .<sup>36</sup> In addition, these species remained on the catalyst surface after cessation of the electric field. Presumably,  $\text{NH}_4^+$  was produced from synthesized  $\text{NH}_3$  and protons. The protons are generated from  $\text{H}_2$  and hop on the catalyst surface when the

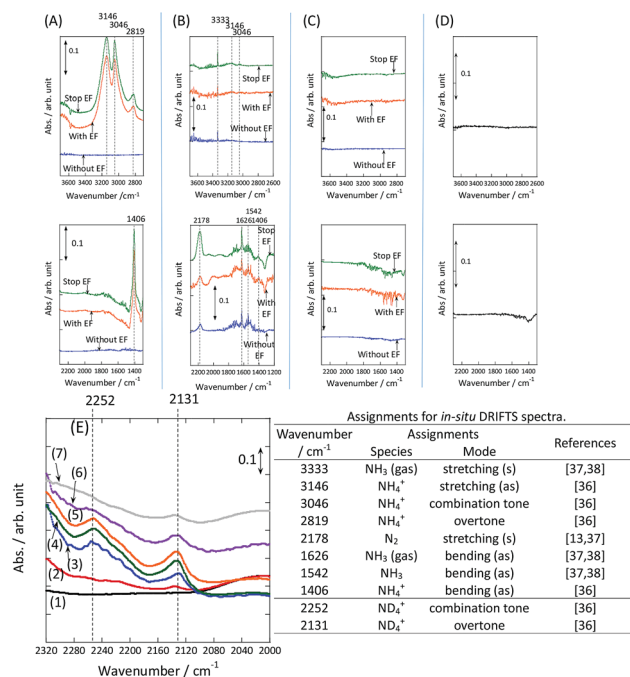


Fig. 3 *In situ* DRIFTS spectra with, without, and after switching off the electric field (EF). (A)  $\text{N}_2$  :  $\text{H}_2$  = 15 : 45 SCCM at 473 K; (B) 10%  $\text{NH}_3$ /He : Ar = 1 : 59 SCCM at 473 K; (C)  $\text{N}_2$  : Ar = 15 : 45 SCCM at 473 K; (D)  $\text{N}_2$  :  $\text{H}_2$  = 15 : 45 SCCM at 648 K (without the EF, catalytic reaction); (E) experiments using an isotope ( $\text{D}_2$ ) at 473 K: (1) after imposing the EF with  $\text{N}_2$  and  $\text{H}_2$ , (2) when  $\text{D}_2$  (15 SCCM) was supplied, (3) when  $\text{D}_2$  was supplied with the EF (10 mA), (4) after imposing the EF with  $\text{D}_2$ , (5) when  $\text{H}_2$  (15 SCCM) was supplied again, (6) when  $\text{H}_2$  was supplied with the EF (10 mA), (7) after imposing the EF with  $\text{H}_2$  and the catalyst (9.9 wt% Cs/5.0 wt% Ru/SrZrO<sub>3</sub>; current, 0, 6, or 10 mA).

electric field is applied. The ammonium cation only exists in a stable form on the catalyst. Fig. 3(E) shows the *in situ* DRIFTS spectra with D<sub>2</sub>. The peaks derived from the isotopes did not appear merely by supplying D<sub>2</sub> to the produced ammonium ions (spectrum 2). However, upon application of the electric field, two peaks assigned to the combination tone and overtone modes of ND<sub>4</sub><sup>+</sup> were observed at around 2252 and 2131 cm<sup>-1</sup> (spectrum 3).<sup>36</sup> These peaks were weakened under H<sub>2</sub> flow conditions in the presence of the electric field (spectrum 6). Based on the above observations, the protons are considered to hop *via* NH<sub>4</sub><sup>+</sup> ions and the catalyst support when the electric field is applied to the catalyst bed. The electric field could not be applied without supplying H<sub>2</sub>. Fig. 3(B) shows the *in situ* DRIFTS spectra while supplying NH<sub>3</sub> at 473 K. Peaks derived from NH<sub>3</sub> and N<sub>2</sub> species were also detected at around 3333, 1626, 1542 and 2178 cm<sup>-1</sup>.<sup>13,37,38</sup> However, peaks assignable to the N-H vibrations derived from NH<sub>4</sub><sup>+</sup> were very weak compared with those in Fig. 3(A), even when applying the electric field. These results show that surface protonics occur only when the forward reaction for ammonia synthesis proceeds in the presence of an electric field.

### Theoretical calculations for ammonia synthesis with/without the electric field and the proposed mechanism of ammonia synthesis in the electric field

To consider the reaction mechanism experimentally and theoretically, we considered the (0001) and (10 $\bar{1}$ 1) facets, which are the exposed facets at the surface of the Ru particles, as observed by the transmission electron microscope (TEM) images in Fig. 4.

To examine how the effect of an electric field on the Ru catalyst can be expressed by theoretical computation, the *in situ* IR spectra of CO adsorbed on Ru/SrZrO<sub>3</sub> were measured (Fig. S3–S6†). The IR spectra with and without an electric field indicate that a blue shift of the CO vibrational frequency occurred when an electric field was applied to the Ru catalyst. Using density functional theory (DFT), the blue shift of the CO vibrational mode was observed to occur when positive charge was introduced into the system, irrespective of the facet and adsorption site (Table S2†). Thus, these results suggest that the effect of an electric field on Ru is well expressed by introducing positive charge into the system.

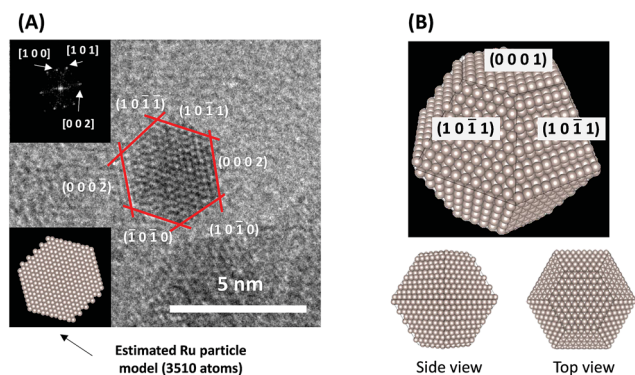
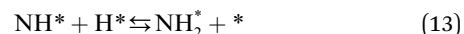
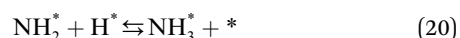


Fig. 4 (A) Representative TEM images of a Ru particle supported on SrZrO<sub>3</sub> and (B) proposed models for the Ru particles.

Next, the ammonia synthesis reaction under an applied electric field was theoretically considered. As suggested by the experimental results, the ammonia synthesis reaction under an applied electric field is significantly different from the conventional catalytic ammonia synthesis reaction, because in the former, protonics govern the reaction. Considering this, both the “dissociative mechanism”,



and the “associative mechanism”,



were examined using theoretical calculations.<sup>39–42</sup> Here, the asterisk (\*) denotes a vacant surface site, and a species with an asterisk is an adsorbed species. The rate-determining steps of the dissociative and associative mechanisms were found to be N<sub>2</sub> dissociation and N<sub>2</sub>H formation, respectively; thus the activation barriers and reaction energies for these two steps were examined.

Using the DFT method, the reaction energies ( $\Delta E$ ) of the N<sub>2</sub> dissociation and N<sub>2</sub>H formation reactions were calculated (Fig. 5). The results show that the application of an electric field, which is simulated by the positive charge in the system, induces an increase in  $\Delta E$  for N<sub>2</sub> dissociation but a decrease in  $\Delta E$  for N<sub>2</sub>H formation. As a result, without an electric field, the formation of N<sub>2</sub>H is an endothermic process but it becomes an exothermic process under an applied electric field. The calculated activation energies ( $E_a$ ) of these processes (Fig. S7(A)†) also indicate that N<sub>2</sub>H is more easily formed when an electric field is applied;  $E_a$  significantly decreased from 0.93 eV (N<sub>2</sub> dissociation) to 0.61 eV (N<sub>2</sub>H formation) when 15 positive charges were introduced into the computational model. Here, the  $E_a$  values on Ru(10 $\bar{1}$ 1) were used because this surface has a larger area in the assumed Ru particle (Fig. 4). This explains the significant decrease of the activation energy with the application of an electric field.





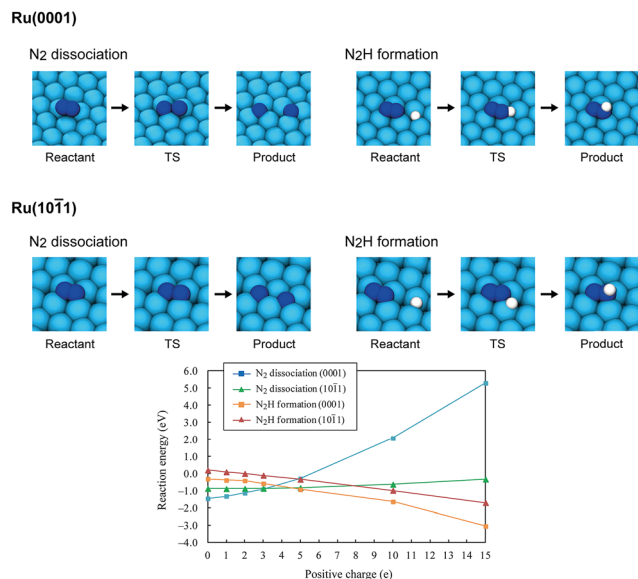


Fig. 5 Optimized structures of the reactant state, transition state (TS) and product state of the  $N_2$  dissociation and  $N_2H$  formation reactions on Ru(0001) and Ru(1011), the reaction energies of the  $N_2$  dissociation and  $N_2H$  formation reactions on Ru(0001) and Ru(1011), and their dependence on the electric field strength, expressed by the magnitude of the positive charge. On Ru(0001), the dissociated N atoms occupy fcc and hcp hollow sites, and  $N_2H$  formation generates  $N_2H$  adsorbed on hcp sites. On Ru(1011), both the dissociated N atoms and generated  $N_2H$  occupy four-fold hollow sites.

In addition to the activation energy, the experimental Arrhenius plot in Fig. 1(B) suggests that the application of an electric field causes a large decrease in the pre-exponential factor. Interestingly, based on transition state theory, the pre-exponential factors for the dissociative and associative mechanisms are very different because they are calculated as

$$A_{\text{diss}} = \frac{k_B T}{h} \frac{q_{\text{TS,diss}}}{q_{N_2}} \quad (22)$$

and

$$A_{\text{asso}} = \frac{k_B T}{h} \frac{q_{\text{TS,asso}}}{q_{N_2} q_{H_2}^{1/2}} \quad (23)$$

respectively, where  $k_B$  and  $h$  are the Boltzmann and Planck constants,  $q_{N_2}$  and  $q_{H_2}$  are the molecular partition functions for  $N_2$  and  $H_2$ , and  $q_{\text{TS,diss}}$  and  $q_{\text{TS,asso}}$  are the molecular partition functions for the transition states of the dissociative and associative mechanisms. The presence of  $q_{H_2}$  in the denominator of eqn (23) makes  $A_{\text{asso}}$  smaller than  $A_{\text{diss}}$  by  $4.5 \times 10^2$ .

Based on these pre-exponential factors and calculated activation energies, a theoretical Arrhenius plot can be constructed (Fig. S7(B)†). Our theoretical plot can explain two important differences between the experimental plots with and without an electric field, when an associative mechanism is assumed for the ammonia synthesis reaction under an applied electric field. Thus, our calculation assuming the associative mechanism explains both the large decreases in  $E_a$  and the pre-exponential factor. This strongly suggests that the ammonia synthesis reaction with and without an electric field proceeds *via* different mechanisms, *i.e.* dissociative and associative mechanisms, respectively.

Our experimental and theoretical investigations demonstrated that proton hopping in an electric field on the catalyst surface plays an important role in  $N_2$  activation at low temperatures. The proposed mechanism for ammonia synthesis in an electric field is presented in Fig. 6. The peculiar surface conduction caused by the electric field, proton hopping, is considered to enable ammonia synthesis to proceed at low temperatures and atmospheric pressure.

## Conclusions

Ammonia synthesis was performed over a 9.9 wt% Cs/5.0 wt% Ru/SrZrO<sub>3</sub> catalyst in an electric field under various pressures. The ammonia synthesis activity of this catalyst increased drastically upon application of the electric field under both atmospheric and 0.9 MPa pressure, even at low reaction temperatures. The maximum ammonia yield per gram of catalyst was  $30\,099 \mu\text{mol g}^{-1} \text{h}^{-1}$ , which is the highest value reported to date. To elucidate the effects of the electric field on ammonia synthesis, a kinetic investigation and *in situ* DRIFTS measurements were conducted under atmospheric pressure. The results of our kinetic analyses demonstrated that both the apparent activation energy and the dependence of the reaction rate on  $N_2$  pressure decreased upon application of the electric field, indicating that clearly different reaction mechanisms occur with and without application of the electric field. Furthermore, isotope exchange tests demonstrated that  $N_2$  dissociative adsorption was markedly promoted by application of the electric field. The *in situ* DRIFTS results revealed that proton conduction *via*  $NH_4^+$  and the catalyst support occurred when the electric field was applied. These unique surface protonics are strongly associated with  $N_2$  activation, which moderates the severe conditions required for ammonia synthesis. The mechanism of ammonia synthesis in an electric field proposed here was also supported by theoretical calculations, demonstrating that the mechanism changed from

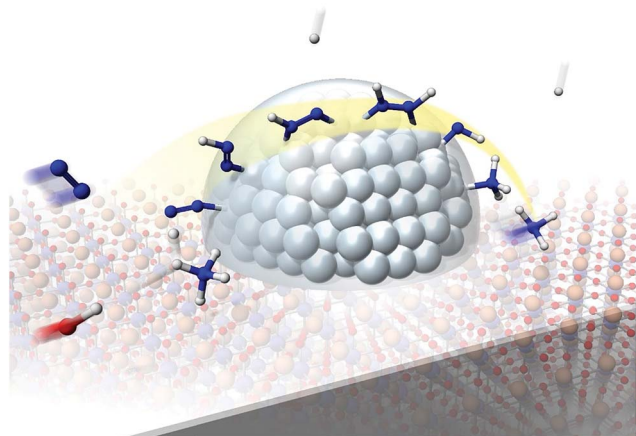


Fig. 6 Schematic illustrating the mechanism of the ammonia synthesis reaction in an electric field.



dissociative to associative upon application of the electric field. In summary, surface protonics induced by the application of an electric field have an important role to play in the enhancement of catalytic ammonia synthesis under mild conditions.

## Acknowledgements

R. M. acknowledges the Leading Graduate Program in Science and Engineering, Waseda University, supported by MEXT, Japan. Analyses of TEM images were mainly conducted by Dr Kei Mukawa. This research was partially supported financially by the JST-CREST.

## References

- 1 U. B. Demirci and P. Miele, *Energy Environ. Sci.*, 2011, **4**, 3334.
- 2 H. Stoltze and J. K. Nerskiv, *Phys. Rev. Lett.*, 1985, **55**(22), 2502.
- 3 C. J. H. Jacobsen, *Chem. Commun.*, 2000, **12**, 1057.
- 4 G. Ertl, *et al.*, *J. Catal.*, 1983, **79**, 359.
- 5 K. Aika, *et al.*, *J. Catal.*, 1972, **27**, 424.
- 6 K. Aika, *et al.*, *J. Catal.*, 1985, **92**, 305.
- 7 O. Hinrichsen, *Catal. Today*, 1999, **53**, 177.
- 8 F. Rosowski, *et al.*, *Appl. Catal., A*, 1997, **151**, 443.
- 9 S. E. Siporin and R. J. Davis, *J. Catal.*, 2004, **225**, 359.
- 10 Z. Wang, *et al.*, *Appl. Catal., A*, 2013, **458**, 130.
- 11 H. Bielawa, *et al.*, *Angew. Chem., Int. Ed.*, 2001, **40**, 1061.
- 12 K. Sato, *et al.*, *Chem. Sci.*, 2017, **8**, 674.
- 13 M. Kitano, *et al.*, *Nat. Chem.*, 2012, **4**, 934.
- 14 M. Kitano, *et al.*, *Nat. Commun.*, 2015, **6**, 1.
- 15 M. Kitano, *et al.*, *Chem. Sci.*, 2016, **7**, 4036.
- 16 Y. Inoue, *et al.*, *ACS Catal.*, 2016, **6**, 7577.
- 17 Y. Tanabe and Y. Nishibayashi, *Coord. Chem. Rev.*, 2013, **257**, 2551.
- 18 K. Arashiba, *et al.*, *Nat. Chem.*, 2011, **3**, 120.
- 19 S. Kuriyama, *et al.*, *Nat. Commun.*, 2016, **7**, 1.
- 20 S. Kuriyama, *et al.*, *Angew. Chem., Int. Ed.*, 2016, **55**, 14291.
- 21 T. Shima, *et al.*, *Science*, 2013, **340**, 1549.
- 22 L. M. Dmitrenko, *et al.*, *Kinet. Catal.*, 1960, **1**, 352.
- 23 K. Aihara, *et al.*, *Chem. Commun.*, 2016, **52**, 13560.
- 24 M. Bai, *et al.*, *Plasma Chem. Plasma Process.*, 2008, **28**, 405.
- 25 H. Uyama and O. Matsumoto, *Plasma Chem. Plasma Process.*, 1989, **9**(1), 13.
- 26 H. Uyama and O. Matsumoto, *Plasma Chem. Plasma Process.*, 1989, **9**(3), 421.
- 27 K. S. Yin and M. Venugopalan, *Plasma Chem. Plasma Process.*, 1983, **3**(3), 343.
- 28 H. Kiyooka and O. Matsumoto, *Plasma Chem. Plasma Process.*, 1996, **16**(4), 547.
- 29 S. Sun, *et al.*, *Appl. Catal., B*, 2017, **200**, 323.
- 30 G. Marnellos and M. Stoukides, *Science*, 1998, **282**, 98–100.
- 31 K. Aika and A. Ozaki, *J. Catal.*, 1969, **13**, 232.
- 32 K. Aika, *et al.*, *Appl. Catal.*, 1986, **28**, 57.
- 33 S. Hagen, *et al.*, *J. Catal.*, 2003, **214**, 327.
- 34 Y. Morikawa and A. Ozaki, *J. Catal.*, 1971, **23**, 97.
- 35 K. Urabe, *et al.*, *J. Catal.*, 1974, **32**, 108.
- 36 E. L. Wagner and D. F. Hornig, *J. Phys. Chem.*, 1950, **18**, 296.
- 37 J. A. Herron, *et al.*, *Surf. Sci.*, 2013, **614**, 64.
- 38 H. Shi, *et al.*, *J. Chem. Phys.*, 1995, **102**, 1432.
- 39 S. Dahl, *et al.*, *Phys. Rev. Lett.*, 1999, **83**(9), 1814.
- 40 K. Honkala, *et al.*, *Science*, 2005, **307**(5709), 555.
- 41 T. H. Rod, *et al.*, *J. Chem. Phys.*, 2000, **112**(12), 5343.
- 42 A. L. Garden and E. Skulason, *J. Phys. Chem. C*, 2015, **119**(47), 26554.

